

ENHANCING MECHANICAL AND CORROSION RESISTANCE OF AISI 304 STAINLESS STEEL WITH DIFFERENT DEGREES OF ROLLING AND USING PLASMA NITRIDING

Renan Matos Monção^{1*}, Wenio Fhará Alencar Borges^{1,2}, Ediones Maciel de Sousa³, Francisco Wlaudy Erimar Lourenço de Araujo Junior⁴, Bruno Alessandro Silva Guedes de Lima⁵, Rafael Marinho Bandeira⁶, Thercio Henrique Carvalho Costa⁷, Francisco Riccely Pereira Feitosa^{4,5}, Romulo Ribeiro Magalhães de Sousa^{1,3}

¹ Federal University of Piauí, Post-graduate Program in Materials Science and Engineering, Teresina, Brazil

renan.matos@ufpi.edu.br

wenio.borges@ifma.edu.br

romulorms@gmail.com

² Federal Institute of Education, Science and Technology of Maranhão, Pedreiras, Brazil

wenio.borges@ifma.edu.br

³ Federal University of Piauí, Post-graduate Program in Physics, Teresina, Brazil

edionesmaciel.36@gmail.com

romulorms@gmail.com

⁴ Federal University of Paraíba, Post-graduate Program Mechanical Engineering, Joao Pessoa, Brazil

wlaudy@hotmail.com

riccellypfeitosa@gmail.com

⁵ Federal University of Paraíba, Center of Technology, Mechanical Engineering Department, Joao Pessoa, Brazil

brunuguedes@gmail.com

riccellypfeitosa@gmail.com

⁶ Federal University of Piauí, Department of Chemistry, Teresina, Brazil

rafael.marinho.bandeira@gmail.com

⁷ Federal University of Rio Grande do Norte, Post-graduate of Mechanical Engineering, Natal, Brazil

thercioc@gmail.com

ABSTRACT

Due to its good corrosion resistance and ductility, 304 stainless steel (304 SS) is a material of choice for various applications. However, its hardness and wear resistance are often not low enough to cater to the demands of highly demanding fields. It is possible to upgrade these characteristics and the life and performance of the parts processed from this material using an established technique, plasma nitriding. This study made a significant contribution to the field by examining the impact of plasma nitriding on 304 SS samples subjected to different degrees of prior rolling, ranging from 0% to 50%. The authors sought to deepen their knowledge of the role of this premodification in nitrogen uptake, the formation of the nitrated phase, and, consequently, the mechanical properties. The characterization methods included X-ray diffraction, scanning electron microscopy, energy-dispersive X-ray spectroscopy, Vickers microhardness, and corrosion resistance tests. The resultant findings confirmed a priori the necessity for a pre-rolling forming pre-treatment of the steel to modify its microstructure and, as a result, the efficiency of the plasma nitriding treatment. As determined by the study, a higher rolling

degree before nitriding results in a higher number of phases that are generated nitrided, and consequently, a higher hardness, wear, and corrosion resistance of the samples with a higher rolling degree is much improved.

KEYWORDS: *AISI 304 steel; Plasma Nitriding; Corrosion; Tribology.*

I. INTRODUCTION

Over the past years, 304 stainless steel (304 SS) has been widely applied in various industrial fields for its superior corrosion resistance, good formability, and high ductility. Nevertheless, the material's wear resistance and surface hardness may be inadequate for some highly demanding applications. Plasma nitriding is a promising process for improving these surface properties, increasing the lifetime performance of components. [1][2]

The effect of plasma nitriding on the mechanical and tribological properties of 304 stainless steel has been previously studied. These researches have shown that the process can significantly improve the material's mechanical resistance and the surface's abrasion. Plasma nitriding can dramatically increase the corrosion resistance of austenitic stainless steels by forming a passivating nitride coating on its surface, i.e., [3][4]

According to the existing research, the early microstructure of the steel may affect the efficiency of the plasma nitriding. As a common pre-treatment, cold rolling has been reported to change the microstructure of 304 stainless steel, leading to morphological changes in the martensite phases and mechanical [properties]. [5] [6]

This relationship has been minimally researched by researchers in the literature, with only a limited number of studies investigating how changes to the degree of previous rolling affect nitrogen absorption, nitrided phase formation, and, thus, material properties. The current work, therefore, performed a complete investigation into the effect of plasma nitriding on samples of 304 stainless steel after different degrees of previous rolling ranging from 0 to 50%.

II. EXPERIMENTAL PROCEDURE

2.1. Sample Preparation

The AISI 304 stainless steel samples were prepared using established and validated procedures from previous studies conducted by the research group. The 304 SS sheets, 10 mm in thickness, were cut into 25 mm x 25 mm plates using a lubricated band saw to prevent thermal changes in the microstructure. This rolling process was carried out using a precision laminator, with the thickness reduction controlled and measured using a high-precision digital micrometer. After the rolling treatment, the samples underwent ultrasonic cleaning in an ethanol solution for 15 minutes to remove any residue or surface contaminants.

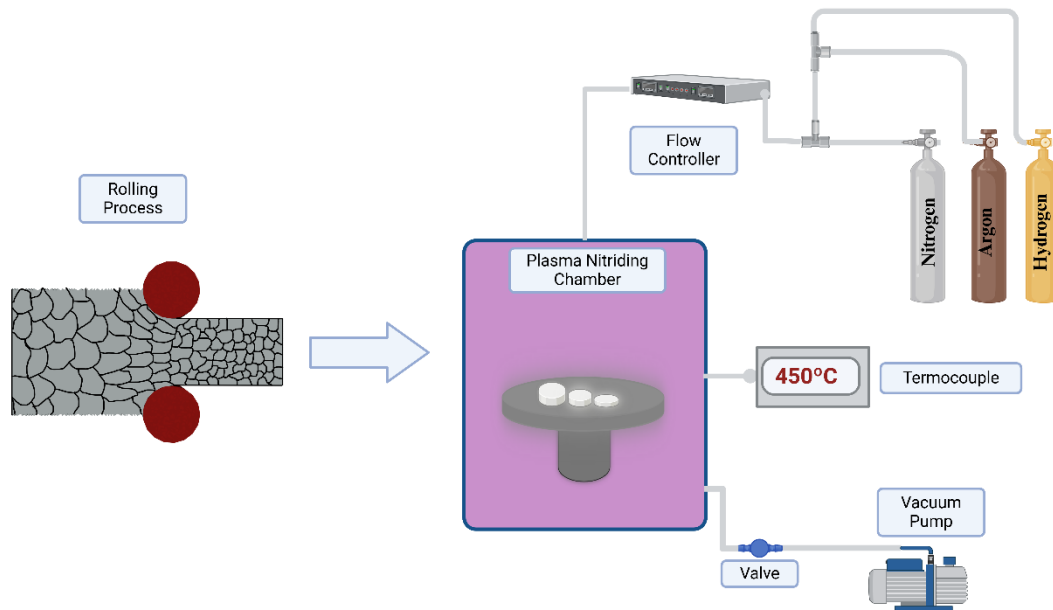


Figure 1. XRD patterns of untreated 304 SS sample and treated at 450°C with different levels of prior rolling.

The samples underwent nitriding at temperatures ranging from 450 to 500 °C for 4 hours, utilizing a gas mixture comprising nitrogen and hydrogen in a 3:1 ratio. The process was conducted under a partial pressure of 3 mbar.

Plasma nitriding was conducted using a well-established protocol that has been shown to effectively improve the surface characteristics of metal alloys based on prior studies by the research team [7][8][9]. The temperature, duration, and gas composition parameters were selected based on prior established values that demonstrated substantial enhancements in hardness and corrosion resistance for the treated samples. This well-validated protocol ensures consistency of the results, enabling direct comparison with the controlled variables investigated in this study.

2.2. Sample Characterization

After the plasma nitriding treatment, the samples underwent characterization to assess the microstructural alterations and mechanical properties. Vickers microhardness testing was conducted, applying a load of 50 gf for 15 s. Five measurements were performed on each sample, and the results were reported as the mean standard deviation. Additionally, scanning electron microscopy was employed to analyze the microstructural changes, with images captured at magnifications of 500x and 2,000x. X-ray diffraction analysis was carried out to identify the phases in the nitrided surface layer, using Cu K α radiation with a step size of 0.02° and a scanning rate of 1°/min. Corrosion resistance was evaluated through tests conducted by the ASTM G5 standard. A three-electrode cell setup was utilized in a sodium chloride solution. Potentiodynamic polarization was performed, sweeping the potential from -250 mV to +250 mV relative to the open circuit potential at a scan rate of 0.167 mV/s. The recorded data was then employed to calculate the corrosion rate based on the measured corrosion current density.

III. RESULTS AND DISCUSSION

The study's findings revealed a significant impact of the prior rolling treatment on the effectiveness of plasma nitriding in enhancing the surface characteristics of 304 stainless steel.

3.1. X-ray Diffraction Analysis

The X-ray diffraction analysis showed that plasma nitriding and different rolling degrees significantly altered the diffraction peaks of 304 stainless steel samples, reflecting microstructural transformations that directly influenced the material's mechanical properties.

The XRD patterns of samples treated at 450 °C (Figure 2) show the predominant presence of austenite (γ -Fe) and ferrite (α -Fe) phases in untreated samples (AR – As Received). As the degree of rolling increased, the intensity of the ferrite peaks progressively intensified relative to the austenite peaks. The literature reports that cold rolling of austenitic stainless steels promotes the formation of martensite phases. [6]

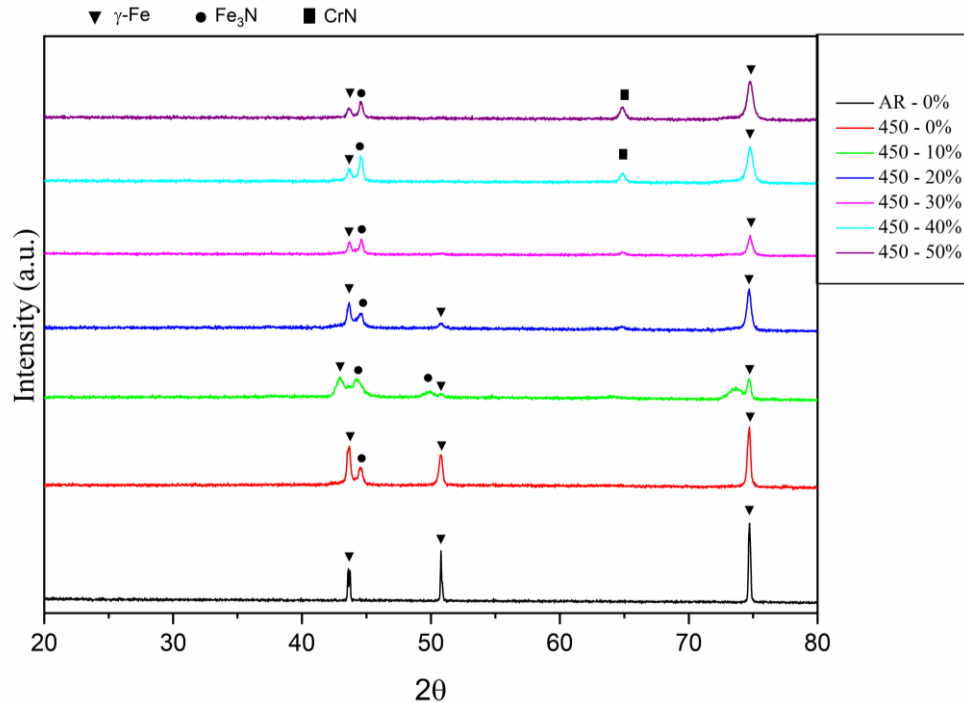


Figure 2. XRD patterns of untreated 304 SS sample and treated at 450°C with different levels of prior rolling.

After plasma nitriding, the XRD patterns revealed the emergence of nitrated phases such as chromium nitride and iron nitride (Fe_3N). The intensity of these nitride peaks significantly increased with higher levels of prior rolling, suggesting that mechanical deformation enhances nitrogen absorption and the formation of nitrated phases.

The peaks at 43° and 44° are characteristic of the austenitic phase (γ -Fe, face-centered cubic structure - FCC). The peak at 44°, present in all samples treated at 450 °C, indicates slight deformation or residual stress in the austenitic phase after nitriding, likely due to nitrogen incorporation and the rolling effect. The austenitic matrix persists, ensuring properties such as toughness and corrosion resistance, while the formation of nitrated phases enhances hardness and wear resistance [10][11]

This finding highlights the persistence of the austenitic matrix, which is crucial for maintaining key properties such as toughness and corrosion resistance. At the same time, the formation of nitride phases enhances the hardness and wear resistance.[12]

The peak around 49° indicates the potential formation of nitrated phases, especially in samples with 10% rolling, demonstrating the influence of mechanical deformation on phase nucleation. Conversely, the gradual reduction of the peak at 51°, characteristic of the austenitic phase, with increasing rolling levels reflects a partial transformation of the austenitic matrix into nitride-rich phases, accompanied by textural changes in the microstructure. [13][14]

The increased intensity of the peak at 64°, observed in samples with higher rolling levels, highlights the formation and growth of phases such as chromium nitride or iron nitride (Fe_3N). The higher defect density favors these hard, wear-resistant phases, such as dislocations introduced by rolling, which act as preferential sites for nucleation and growth.[15][16]

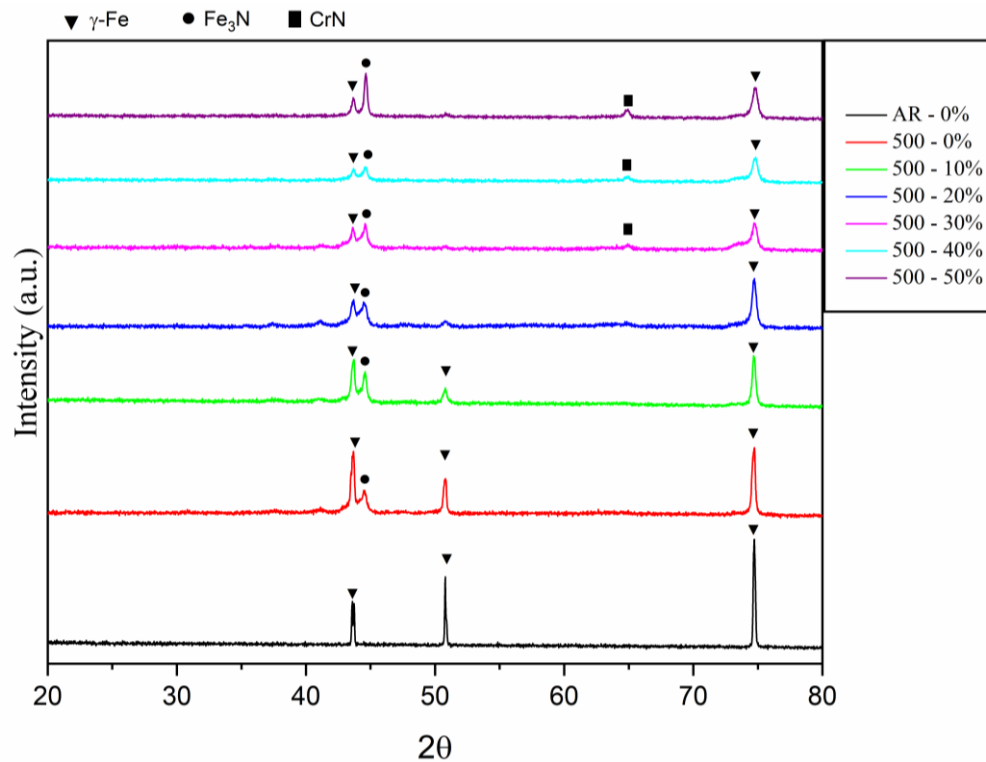


Figure 3. XRD patterns of untreated 304 SS sample and treated at 500°C with different levels of prior rolling.

The XRD patterns obtained from samples treated at 500 °C (Figure 3) exhibited a more prominent presence of the austenitic phase, indicating its enhanced thermal stability at the higher nitriding temperature. A slight shift of the peak at 44° towards higher angles was observed, suggesting the introduction of deformation or residual stresses within the crystalline structure. This shift can be attributed to the combined impact of the rolling pre-treatment and the heat exposure during the plasma nitriding process.

The intensification of the peaks at 64°, corresponding to nitrided phases, was more evident in samples with higher rolling levels. This reflects the enhanced formation of hard, wear-resistant nitrides, such as chromium and iron nitrides, within the deformed steel matrix.

Comparatively, samples treated at 450 °C exhibited a more pronounced transformation of the austenitic matrix, evidenced by the reduction in austenite peak intensity and the significant emergence of nitride peaks. This behavior is attributed to the increased defect density introduced by rolling, which promotes the nucleation and growth of nitrided phases.

Furthermore, at both treatment temperatures, the peak intensity at 51°, characteristic of the austenitic phase, progressively decreased with higher rolling levels. This confirms the gradual transformation of the austenitic matrix into nitride-enriched phases, altering the overall crystalline structure of the steel.

3.2. Scanning Electron Microscopy Analysis

The scanning electron microscopy analysis of plasma nitrided 304 stainless steel samples subjected to varying degrees of prior rolling at 450 °C (Figure 3) revealed a notable correlation between mechanical rolling and the thickness of the nitrided layers. The quantitative data showed that the nitrided layer thicknesses were approximately $4.439 \pm 0.249 \mu\text{m}$ for the unrolled sample, $5.568 \pm 0.774 \mu\text{m}$ for the sample with 10% rolling, and $5.327 \pm 0.224 \mu\text{m}$ for the sample with 20% rolling.

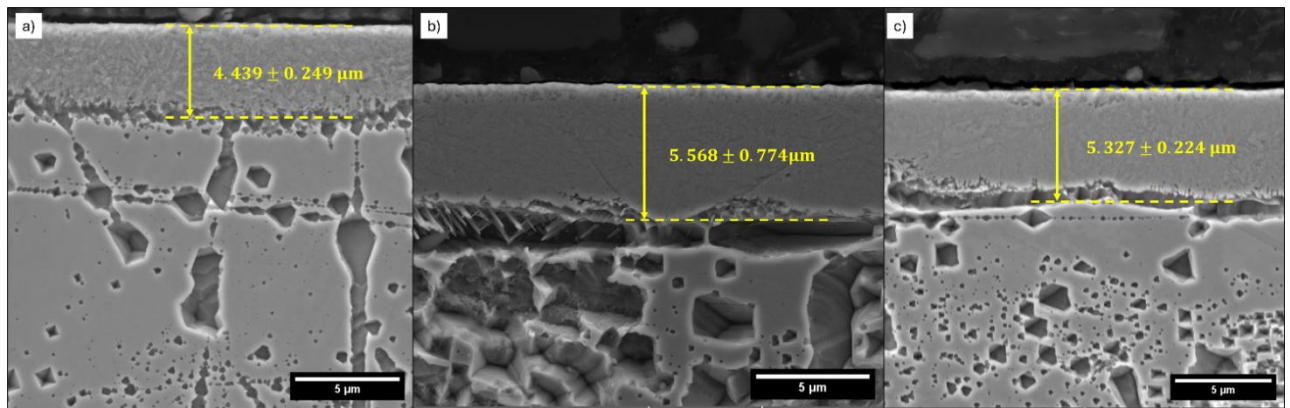


Figure 4. SEM images of the treated 304 SS samples: (a) 0%, 450 °C; (b) 10%, 450 °C; (c) 20%, 450 °C.

The scanning electron microscopy analysis of plasma nitrided 304 stainless steel samples subjected to varying degrees of prior rolling at 450 °C (Figure 4) revealed a notable correlation between mechanical rolling and the thickness of the nitrided layers. The quantitative data showed that the nitrided layer thicknesses were approximately $4.439 \pm 0.249 \mu\text{m}$ for the unrolled sample, $5.568 \pm 0.774 \mu\text{m}$ for the sample with 10% rolling, and $5.327 \pm 0.224 \mu\text{m}$ for the sample with 20% rolling.

The detailed analysis of the measurements indicates that rolling enhances nitrogen absorption and restructures the material's microstructure. This can be attributed to the facilitation of nitrogen diffusion on the surface due to the mechanical deformation from the rolling process. As a result, there is a trend of increasing nitrided layer thickness with higher rolling degrees, up to the point of stabilization or slight decrease, as observed in the sample with 20% rolling.[17][18]

The samples' XRD analysis further supports the SEM observations, with the changes in the diffraction peaks indicating that the treatments induced microstructural modifications. Specifically, the characteristic peaks of the austenitic and nitride phases reflect a varied incorporation of nitrogen and a reorganization of the crystalline structure, which are directly influenced by the degree of mechanical deformation.

The SEM micrographs also reveal a distinct nitrided compound layer and a diffusion zone, with the compound layer exhibiting a higher density of nitride precipitates. The thickness of the compound layer and the diffusion zone, along with the analysis of a gradual transition between them, suggest that the mechanically induced defects and dislocations contributed to the enhanced nitrogen absorption and the formation of nitrided phases.[18][19]

Material microstructure changes play an important role in its mechanical and corrosion properties. Based on microhardness analysis, the treated samples showed a significant hardness increase in contrast to the untreated sample due to the formation of hard nitrides on the surface. Specifically, testing the corrosion resistance using potentiodynamic polarization curves showed increased corrosion protection for the samples with increased rolling degrees. This implies that the combination of nitriding and rolling improves the mechanical performance and the material's chemical stability in corrosive environments.

3.3. Vickers Microhardness Analysis

The microhardness data (Figure 5) for the 500 °C treated samples demonstrates a substantial increase in surface hardness compared to the untreated material. The untreated 304 stainless steel sample exhibited an average microhardness of 245.48 HV. Following the plasma nitriding treatments, the microhardness increased progressively with the degree of nitriding. Specifically, the sample with 0% nitriding had a microhardness of 509.56 HV, while the 50% nitrided sample reached a significantly higher value of 740.95 HV.

The significant increase in surface microhardness can be attributed to the formation of hard nitride phases, as evidenced by the XRD peaks observed at 49° and 64° , which correspond to iron nitrides and potential chromium nitrides. Notably, the stability of the peaks at 43° and 44° , characteristic of the austenitic phase, suggests that the austenitic matrix remains intact mainly during the nitriding process.

This preservation of the austenitic structure ensures that the material retains its toughness and corrosion resistance. At the same time, the formation of the hard nitride phases contributes to the substantial enhancement in surface hardness.[18].

The reduction in the intensity of the peak at 51° with increasing degrees of nitriding suggests a partial transformation of the austenitic matrix into harder, nitrogen-rich phases. This is probably the consequence of the increased introduction of nitrogen and the deformation caused by the nitriding process. Furthermore, the increase of the peak at 64° with increasing nitridation levels reflects the nature of nitride phases and, hence, the benefits of the enhanced surface hardness observed. [20][21]

The samples treated at 450°C also exhibited an increase in microhardness compared to the untreated material, which had an average microhardness of 245.48 HV. Specifically, the sample with 0% nitriding registered a microhardness of 339.29 HV, while the sample with 50% nitriding reached 733.46 HV. Even with the significant increase, the average microhardness was slightly lower than that processed for the samples submitted to 500°C , implying that higher temperatures promote more effective diffusion of nitrogen and the development of stronger nitride phases.

X-ray diffraction studies on the 450°C treated samples revealed faint and sharp peaks at 43° and 44° of the austenitic phase, implying a lower degree of stability of the austenitic phase in the 450°C treated samples compared with the case of the 500°C treated samples. Additionally, the induration process of the grown nitrides was also observed to a lower extent, indicating that the temperature of 450°C was less effective than that of 500°C in producing these soft phases.

The comparative study indicates that by applying 500°C heat treatment of the NTH surface, due to preferential nitride phase formation, the surface microhardness of the ceramic is enhanced; consequently, the ceramic surface is harder. This is corroborated by the X-ray diffraction data, which demonstrate increased intensity of nitride-related peaks and a more significant decrease in austenitic phase peaks for the samples treated at the higher temperature.

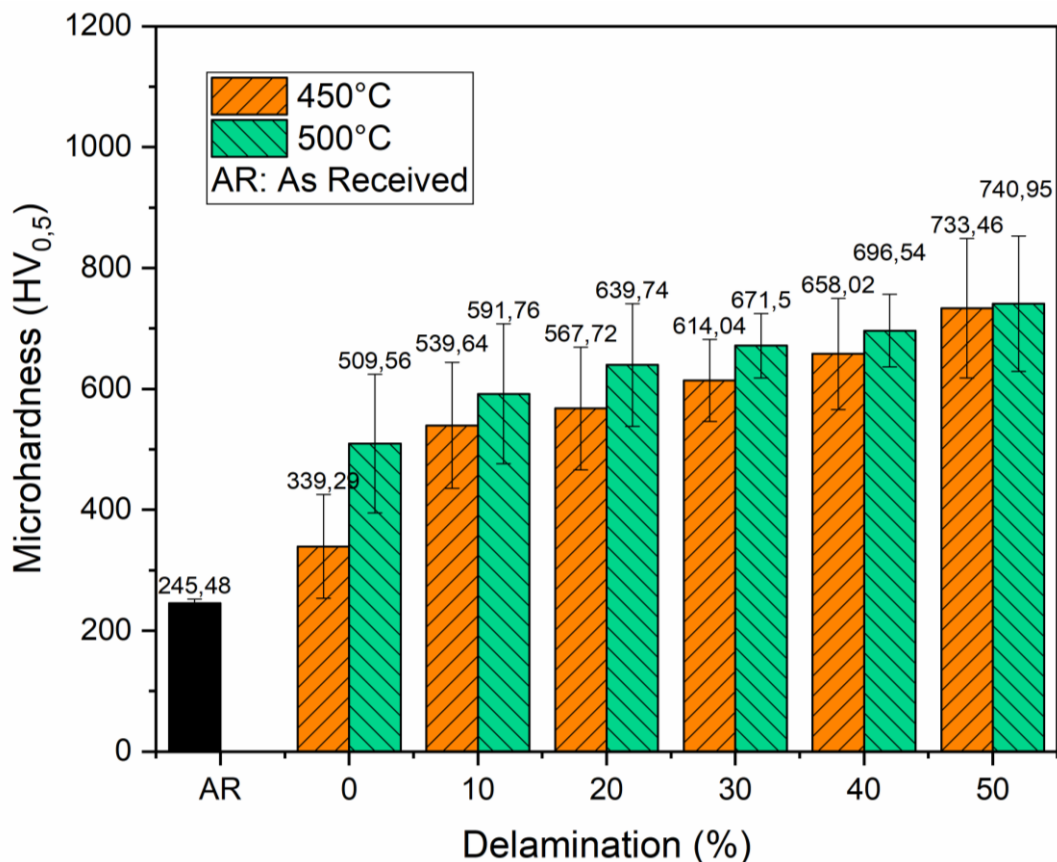


Figure 5. Vickers microhardness measured on the surface of the untreated and treated 304 SS samples.

3.4. Corrosion Resistance Evaluation

Figure 6 shows the potentiodynamic polarization curves of 304 SS samples subjected to rolling and heat treatment at 450 °C and 500 °C. Samples corresponding to 0% rolling must be understood as non-rolled samples used in the study to compare results. The potential sweep occurred in the anodic direction of the potentiodynamic polarization curves, ending when the current density values reached $1 \text{ mA} \cdot \text{cm}^{-2}$. In general, the profiles of the potentiodynamic polarization curves are similar. This demonstrates that the nature of the corrosion process is also similar between different samples. However, there are differences to be observed, which will be pointed out primarily to samples subjected to heat treatment at 450 °C. [22]

The cathodic curves showed much more similar behavior than the anodic branches of the potentiodynamic polarization curves. Figure 6a indicates that the sample heat-treated at 450 °C and rolled 10% presented the corrosion potential (E_{Corr}) more displaced in the cathodic direction, $E_{\text{Corr}} = -500 \text{ mV}$, than the others. The corrosion potential values of all electrodes are shown in Table 1. With the increase in rolling to 20%, the corrosion potential shifts to a more anodic region, indicating an improvement in the alloy's protection condition. Furthermore, the sample with 20% rolling and heat treated at 450 °C exhibited a decrease in corrosion current density (j_{Corr}). The j_{Corr} values, as well as the corrosion rate, are also included in Table 1. Samples treated at 450 °C and rolled from 30% to 50% exhibited $E_{\text{Corr}} \approx -427 \text{ mV}$. The corrosion potentials of these samples are around 20 mV, which is more negative than that of the non-rolled sample, $E_{\text{Corr}} = -404 \text{ mV}$; that is, they present similar conditions of susceptibility to corrosion. Notably, the 40% and 50% rolled samples presented lower j_{Corr} values, even lower values than the non-rolled sample. The 50% rolled steel electrode presented the lowest corrosion current density value, being $j_{\text{Corr}} = 2.45 \mu\text{A} \cdot \text{cm}^{-2}$.

Figure 6b shows the potentiodynamic polarization curves of steel electrodes without rolling, rolled up to 50%, and treated at 500 °C. The electrodes show greater differences in the anode curves. The 30% and 40% rolled samples presented less negative corrosion potentials than the others, $E_{\text{Corr}} = -370 \text{ mV}$ and $E_{\text{Corr}} = -355 \text{ mV}$, respectively. In this case, there was an improvement in the corrosion potentials of 58 mV and 71 mV between the samples rolled at 30% and 40% and heat treated at 450 °C and 500 °C. Thus, increasing the temperature in the sample treatment process improves corrosion protection. These samples also presented lower j_{Corr} values than the others, emphasizing the 40% rolled sample, which had $j_{\text{Corr}} = 0.45 \mu\text{A} \cdot \text{cm}^{-2}$.

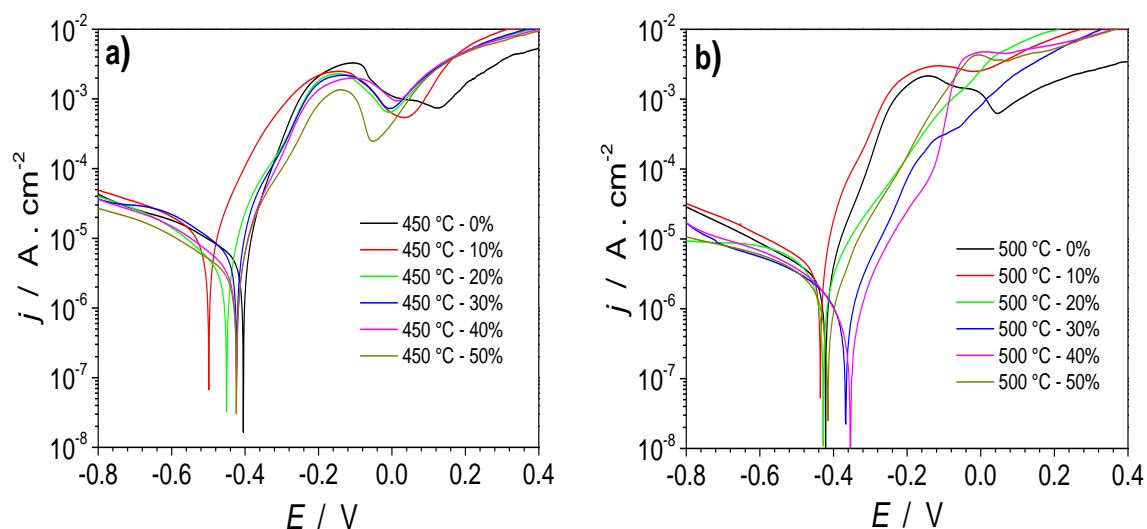


Figure 6. 304 SS samples subjected to different rolling percentages ranging from 0% to 50%. Samples were: (a) heat treated at 450 °C and (b) heat treated at 500 °C.

Table 1. Parameters extracted from the potentiodynamic polarization curves from Tafel extrapolation.

Sample		E_{Corr} (mV)	j_{Corr} ($\mu\text{A} \cdot \text{cm}^{-2}$)	Corrosion Rate ($\times 10^{-2} \text{ mm} \cdot \text{yr}^{-1}$)
Temperature ($^{\circ}\text{C}$)	Delamination (%)			
450 $^{\circ}\text{C}$	0	-404	5.14	5.3
	10	-500	9.13	9.5
	20	-452	3.67	3.8
	30	-428	5.32	5.5
	40	-426	3.20	3.3
	50	-427	2.45	2.5
500 $^{\circ}\text{C}$	0	-414	2.54	2.6
	10	-440	3.93	4.1
	20	-430	1.93	2.0
	30	-370	0.81	0.8
	40	-355	0.45	0.5
	50	-412	0.79	0.8

Figure 7 shows the corrosion rate values of the different samples subjected to potentiodynamic polarization curves. The corrosion current density values were obtained from Tafel extrapolation of the polarization curves and used to calculate the corrosion rate by ASTM G102 – 89. Results indicate that the non-rolled sample has a higher corrosion rate than the others, except for the 10% rolled sample. The 10% rolling condition showed the highest corrosion rate at the two treatment temperatures used for 304 SS.

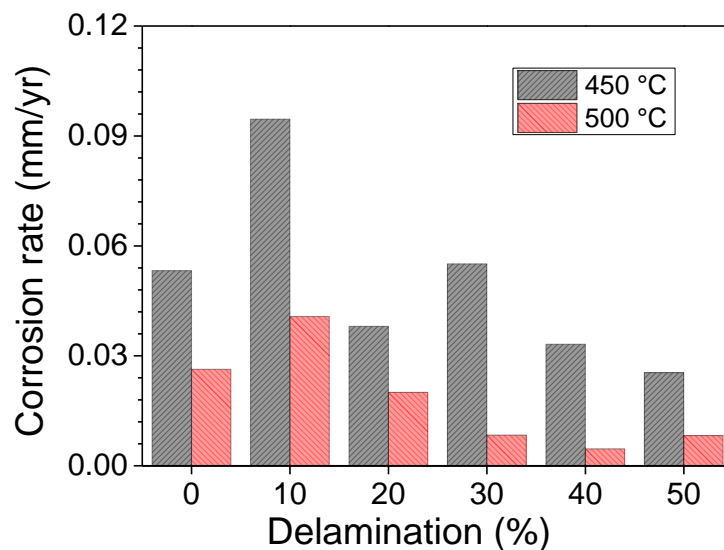


Figure 7. Corrosion rate of 304 SS samples subjected to different rolling percentages ranging from 0% to 50%. The samples were heat treated at 450 $^{\circ}\text{C}$ and 500 $^{\circ}\text{C}$.

On the other hand, those sampled with higher rolling percentages, for example, 30% to 50%, showed the lowest corrosion rates. It is worth noting that the 40% rolled sample treated at 500 $^{\circ}\text{C}$ exhibited the lowest corrosion rate, being $5 \times 10^{-3} \text{ mm} \cdot \text{yr}^{-1}$. This value is almost seven times lower than the corrosion rate of the 40% rolled sample treated at 450 $^{\circ}\text{C}$. Therefore, the influence of the temperature used to treat the samples on the corrosion resistance of 304 SS is notable.

Therefore, increasing rolling up to 50%, associated with the increase in the temperature at which the heat treatment is carried out, promotes improvement in the corrosion resistance properties of 304 SS. Thus, when associated with adequate heat treatment, the rolling process favors the application of rolled steel, as in the case of 304 SS.

IV. CONCLUSIONS

This study investigated the impacts of plasma nitriding on 304 stainless steel samples subjected to varying degrees of prior rolling, aiming to optimize the mechanical and corrosion resistance characteristics for industrial use. The key findings can be summarized as follows.

Plasma nitriding, conducted under various rolling conditions, significantly impacted the microstructure and surface characteristics of 304 stainless steel. The findings indicate that elevating the degree of rolling prior to nitriding promoted the formation of nitrided phases, contributing to enhanced hardness and wear resistance.

The X-ray diffraction analyses revealed that as the degree of prior rolling increased, the formation of nitride phases intensified. This demonstrates a direct relationship between the extent of rolling and the effectiveness of plasma nitriding in altering the treated surface's microstructure.

Scanning electron microscopy analyses revealed the layer structures formed by plasma nitriding, with the thickness and the morphology of the layers being influenced by the degree of prior rolling.

Vickers microhardness evaluations demonstrated that plasma nitriding enhanced surface hardness across all samples, with the most substantially improved hardness observed in the samples with the highest degrees of prior rolling. This highlights the critical role of pre-rolling treatment in optimizing the efficacy of the subsequent surface treatment.

Corrosion resistance evaluations revealed that while all treated samples demonstrated enhanced performance compared to the untreated sample, specimens with greater degrees of prior rolling exhibited lower corrosion current densities, implying improved resistance to environmental degradation.

The findings of this comprehensive study show that the synergistic effects of prior rolling and plasma nitriding can be leveraged to significantly enhance the microstructural, mechanical, and corrosion resistance properties of 304 stainless steel, paving the way for improved performance and extended service life in industrial applications.

ACKNOWLEDGEMENTS

We are grateful to the Plasma Laboratory - LABPLASMA (UFPI), the Interdisciplinary Center for Advanced Materials - LIMAV (UFPI/MCTI/FINEP), the Post-Graduate Program of Mechanical Engineering (PPGEM-UFPPB) and the Post-Graduate Program of Materials Science and Engineering (PPGCM-UFPI) for technical support. This research was funded by the Brazilian National Council for Scientific and Technological Development (CNPq) for the master's scholarship, grant number 307181/2022-7.

REFERENCES

- [1] Ren, X., Yang, W., He, L., Li, D., & Yuan, J. (2022). Effect of Expansion Deformation on the Mechanical Properties and Corrosion Resistance of an AISI 304 Stainless Steel Tube in Water from an Oilfield. In X. Ren, W. Yang, L. He, D. Li, & J. Yuan, *Coatings* (Vol. 12, Issue 10, p. 1415). Multidisciplinary Digital Publishing Institute. <https://doi.org/10.3390/coatings12101415>
- [2] Amininejad, A., Jamaati, R., & Hosseinipour, S. J. (2020). Improvement of strength-ductility balance of SAE 304 stainless steel by asymmetric cross rolling. In A. Amininejad, R. Jamaati, & S. J. Hosseinipour, *Materials Chemistry and Physics* (Vol. 256, p. 123668). Elsevier BV. <https://doi.org/10.1016/j.matchemphys.2020.123668>
- [3] Huang, Z., Guo, Z.-X., Liu, L., Guo, Y., Chen, J., Zhang, Z., Li, J., Li, Y., Zhou, Y., & Liang, Y.-S. (2020). Structure and corrosion behavior of ultra-thick nitrided layer produced by plasma nitriding of austenitic stainless steel. In Z. Huang, Z.-X. Guo, L. Liu, Y. Guo, J. Chen, Z. Zhang, J. Li, Y. Li, Y. Zhou, & Y.-S. Liang, *Surface and Coatings Technology* (Vol. 405, p. 126689). Elsevier BV. <https://doi.org/10.1016/j.surfcoat.2020.126689>
- [4] Díaz-Guillén, J. C., Naeem, M., Acevedo-Dávila, J. L., Hdz-García, H. M., Iqbal, J., Khan, M. A., & Mayén, J. (2020). Improved Mechanical Properties, Wear and Corrosion Resistance of 316L Steel by Homogeneous Chromium Nitride Layer Synthesis Using Plasma Nitriding. In J. C. Díaz-Guillén, M. Naeem, J. L. Acevedo-Dávila, H. M. Hdz-García, J. Iqbal, M. A. Khan, & J. Mayén, *Journal of Materials Engineering and Performance* (Vol. 29, Issue 2, p. 877). Springer Science+Business Media. <https://doi.org/10.1007/s11665-020-04653-9>

- [5] Li, L., Liu, R., Liu, Q., Wu, Z., Meng, X., & Fang, Y. (2022). Effects of Initial Microstructure on the Low-Temperature Plasma Nitriding of Ferritic Stainless Steel. In L. Li, R. Liu, Q. Liu, Z. Wu, X. Meng, & Y. Fang, *Coatings* (Vol. 12, Issue 10, p. 1404). Multidisciplinary Digital Publishing Institute. <https://doi.org/10.3390/coatings12101404>
- [6] He, S., & Jiang, D. (2018). Effect of the Degree of Rolling Reduction on the Stress Corrosion Cracking Behavior of SUS 304 Stainless Steel. In S. He & D. Jiang, *International Journal of Electrochemical Science* (Vol. 13, Issue 2, p. 1614). Elsevier BV. <https://doi.org/10.20964/2018.02.56>
- [7] Costa, E. da S., Sousa, R. R. M. de, Monção, R. M., Libório, M. S., & Costa, T. H. de C. (2021). Nitretação e deposição por plasma em ferramentas de aços AISI M2 e D2 utilizadas na conformação e estampagem de pregos: um estudo de viabilidade. In E. da S. Costa, R. R. M. de Sousa, R. M. Monção, M. S. Libório, & T. H. de C. Costa, *Matéria* (Rio de Janeiro) (Vol. 26, Issue 1). Federal University of Rio de Janeiro. <https://doi.org/10.1590/s1517-707620210001.1222>
- [8] Furtado, A. S. A., Neto, J. R. de B., Serra, P. L. C., & Sousa, R. R. M. de. (2020). Processamento de aço API 5L X70 por laminação a morno e nitretação a plasma. In A. S. A. Furtado, J. R. de B. Neto, P. L. C. Serra, & R. R. M. de Sousa, *Matéria* (Rio de Janeiro) (Vol. 25, Issue 2). Federal University of Rio de Janeiro. <https://doi.org/10.1590/s1517-707620200002.1040>
- [9] Serra, P. L. C., Neto, J. R. de B., Furtado, A. S. A., Sampaio, W. R. V., Feitor, M. C., Costa, T. H. de C., & Sousa, R. R. M. de. (2020). Estudo de nitretação a plasma e tratamento duplex em brocas de aço rápido. In P. L. C. Serra, J. R. de B. Neto, A. S. A. Furtado, W. R. V. Sampaio, M. C. Feitor, T. H. de C. Costa, & R. R. M. de Sousa, *Matéria* (Rio de Janeiro) (Vol. 25, Issue 2). Federal University of Rio de Janeiro. <https://doi.org/10.1590/s1517-707620200002.1072>
- [10] Borgioli, F. (2020). From Austenitic Stainless Steel to Expanded Austenite-S Phase: Formation, Characteristics and Properties of an Elusive Metastable Phase. In F. Borgioli, *Metals* (Vol. 10, Issue 2, p. 187). Multidisciplinary Digital Publishing Institute. <https://doi.org/10.3390/met10020187>
- [11] Che, H. L., Christiansen, T. L., Lei, M. K., & Somers, M. A. J. (2022). Co-existence of γ' N phase and γ N phase in nitrided austenitic Fe-Cr-Ni alloys - II: A pragmatic modeling approach. In H. L. Che, T. L. Christiansen, M. K. Lei, & M. A. J. Somers, *Acta Materialia* (Vol. 235, p. 118094). Elsevier BV. <https://doi.org/10.1016/j.actamat.2022.118094>
- [12] Maznichenovsky, A. N., Сприкут, P. B., & Goikhenberg, Y. N. (2020). Investigation of Nitrogen Containing Austenitic Stainless Steel. In A. N. Maznichenovsky, P. B. Сприкут, & Y. N. Goikhenberg, *Materials science forum* (Vol. 989, p. 152). Trans Tech Publications. <https://doi.org/10.4028/www.scientific.net/msf.989.152>
- [13] Mucsi, A. (2018). Effect of hot rolling conditions on the nitride precipitation process in low carbon steel strips. In A. Mucsi, *IOP Conference Series Materials Science and Engineering* (Vol. 426, p. 12036). IOP Publishing. <https://doi.org/10.1088/1757-899x/426/1/012036>
- [14] Fernandes, F. M. B., Mändl, S., Oliveira, R. M., & Ueda, M. (2014). Mechanical properties of nitrogen-rich surface layers on SS304 treated by plasma immersion ion implantation. In F. M. B. Fernandes, S. Mändl, R. M. Oliveira, & M. Ueda, *Applied Surface Science* (Vol. 310, p. 278). Elsevier BV. <https://doi.org/10.1016/j.apsusc.2014.04.142>
- [15] Liu, G., Sun, H., Wang, E., Sun, K., Zhu, X., & Fu, Y. (2021). Effect of Deformation on the Microstructure of Cold-Rolled TA2 Alloy after Low-Temperature Nitriding. In G. Liu, H. Sun, E. Wang, K. Sun, X. Zhu, & Y. Fu, *Coatings* (Vol. 11, Issue 8, p. 1011). Multidisciplinary Digital Publishing Institute. <https://doi.org/10.3390/coatings11081011>
- [16] Jeon, J. B., & Chang, Y. W. (2017). Effect of Nitrogen on Deformation-Induced Martensitic Transformation in an Austenitic 301 Stainless Steels. In J. B. Jeon & Y. W. Chang, *Metals* (Vol. 7, Issue 11, p. 503). Multidisciplinary Digital Publishing Institute. <https://doi.org/10.3390/met7110503>
- [17] Sun, S., Mu, J., Jiang, Z., Ji, C., Lian, J., & Jiang, Q. (2013). Effect of cold rolling on tensile properties and microstructure of high nitrogen alloyed austenitic steel. In S. Sun, J. Mu, Z. Jiang, C. Ji, J. Lian, & Q. Jiang, *Materials Science and Technology* (Vol. 30, Issue 2, p. 146). Maney Publishing. <https://doi.org/10.1179/1743284713y.0000000422>
- [18] Biehler, J., Hoche, H., & Oechsner, M. (2017). Nitriding behavior and corrosion properties of AISI 304L and 316L austenitic stainless steel with deformation-induced martensite. In J. Biehler, H. Hoche, & M. Oechsner, *Surface and Coatings Technology* (Vol. 324, p. 121). Elsevier BV. <https://doi.org/10.1016/j.surfcoat.2017.05.059>

- [19] Sun, S., Sun, G., Jiang, Z., Ji, C., Liu, J.-A., & Lian, J. (2014). Effects of cold rolling deformation on microstructure, hardness, and creep behavior of high nitrogen austenitic stainless steel. In S. Sun, G. Sun, Z. Jiang, C. Ji, J.-A. Liu, & J. Lian, *Chinese Physics B* (Vol. 23, Issue 2, p. 26104). IOP Publishing. <https://doi.org/10.1088/1674-1056/23/2/026104>
- [20] Wang, B., Lv, Z., Zhou, Z., Sun, S., Huang, X., & Fu, W. T. (2015). Combined effect of rapid nitriding and plastic deformation on the surface strength, toughness and wear resistance of steel 38CrMoAlA. In B. Wang, Z. Lv, Z. Zhou, S. Sun, X. Huang, & W. T. Fu, *IOP Conference Series Materials Science and Engineering* (Vol. 89, p. 12046). IOP Publishing. <https://doi.org/10.1088/1757-899x/89/1/012046>
- [21] Naeem, M., Iqbal, J., Zakaullah, M., Shafiq, M., Zaka-ul-Islam, M., Díaz-Guillén, J. C., López-Badillo, C. M., Sousa, R. R. M. de, & Khan, M. A. (2019). Enhanced wear and corrosion resistance of AISI-304 steel by duplex cathodic cage plasma treatment. In M. Naeem, J. Iqbal, M. Zakaullah, M. Shafiq, M. Zaka-ul-Islam, J. C. Díaz-Guillén, C. M. López-Badillo, R. R. M. de Sousa, & M. A. Khan, *Surface and Coatings Technology* (Vol. 375, p. 34). Elsevier BV. <https://doi.org/10.1016/j.surfcoat.2019.07.012>
- [22] Baranidharan, K., S., T. K., Uthayakumar, M., & Parameswaran, P. (2021). Comprehensive review of various corrosion behaviours on 316 stainless steel. In K. Baranidharan, T. K. S., M. Uthayakumar, & P. Parameswaran, *Metallurgical and Materials Engineering*. Association of Metallurgical Engineers of Serbia. <https://doi.org/10.30544/570>